American Journal of Neurology Research

Research Article

A Clinical, Immunohistochemical, Doble Fluoresce Immunostaining and Ultrastructure Analysis of Papillary Craniopharyngioma

Martha Lilia Tena-Suck[1*], Alma Ortiz-Plata[2], Wilhem Moreno[3], Citlaltepetl Salinas-Lara[1], Carlos Sánchez-Garibay[1], Sergio Zavala-Vega[1] and María del Carmen Rubio[1]

[1]*Departamento de Neuropatología. Instituto Nacional de Neurología y Neurocirugía. Manuel Velasco Suarez, ciudad de México.*

[2]*Laboratorio de Neuropatología Experimental. Instituto Nacional de Neurología y Neurocirugía. Manuel Velasco Suarez, ciudad de México.*

[3]*Laboratorio de Neurofisiología. Instituto Nacional de Neurología y Neurocirugía. Manuel Velasco Suarez, ciudad de México.*

Corresponding Author Information

Martha Lilia Tena -Suck M.D
Departamento de Neuropatología, Instituto Nacional de Neurología y Neurocirugía, Manuel Velasco Suarez, ciudad de México, Av. Insurgentes sur no 3877, colonia la joya, alcaldía de Tlalpan, Ciudad de México, México, Tel: +525556063822 ext. 2011.

Received: January 03, 2023; **Accepted:** January 31, 2023; **Published:** February 04, 2023

Citation: Tena-Suck ML, Ortiz-Plata A, Moreno W, et al,. A Clinical, Immunohistochemical, Doble Fluoresce Immunostaining and Ultrastructure Analysis of Papillary Craniopharyngioma. American J Neurol Res. 2023; 2(1):1-4.

ABSTRACT

Background: Craniopharyngioma is epithelial tumor located in the parasellar region, classified into histopathologically, genetically, clinically and prognostically as adamantinomatous and papillary subtypes

Aim: A descriptive design, to determine the immunohistochemical expression of BRAFV600E, β-catenin, E-cadherin, clau1- 5, occludin, TNFα, IL6,10,20, gal-1,3,9 and Glut-3, 4, βFGF, IGF, EGFR, DPGF, Ki-67li and MVD in PaCPs.

Materials and Methods: clinic, pathological immunostaining and ultrastructure correlation on paraffin embedded tissue sections of 13 cases of papillary craniopharyngioma.

Results: Results. 10 (77%) male and 3 (23%) females, 8 (62%) recurrence and 5(39%) did not. 6 had a cystic appearance, 6 with atypia, 7 with squamous metaplastic changes with foamy macrophages and inflammation. Those who recurred presented higher indices of Ki67 and MVD, CK7, glut3, Gal3, Il6, Il20, and CD68 overexpression. BRAFv600E was doble immunofluorescence coexpresed with Il6, β-catenin, and TNFα as well as lower expression of E-cadherin, β-catenin, occludin, than those who did not recur. Likewise, by EM vacuole binding proteins, glycogen deposits and an increase in microgranules and loss of desmosomes observed. Opening or loss of intercellular adhesions. Pa CPs also presents paracrine secretion and probably lead to OMF production.

Discussion: We observed a correlation with the expression of BRAFV600E with higher Ki-67Li and MVD, strong expression of growth factors, glucose transport galectins, inflammatory factor and loss of membranal TJ proteins expressed in epithelial cells. With they play an important role in cell polarity and cell adhesion, brain invasion as well as, in maintaining paracellular barrier functions, paracrine secretion and senesce.

Keywords

Craniopharyngioma, Craniopharyngiomas, Papillary craniopharyngiomas, β-Catenin.

Abbreviation

CPs: Craniopharyngiomas, AdaCP: Adamantinomatous craniopharyngioma, PaCP: Papillary Craniopharyngioma, IHC: Immunohistochemistry, INNN: National Institute of Neurology and Neurosurgery of Mexico City, CF: Cyst formation, SM: Squamous Metaplasia, SP: Solid Pattern, BI: Brain Invasion, BCFVC: Internal portion or Basal cells of the Vascularized Fibroconnective Core, FFP: Formalin Fixed and Paraffin embedded, CK7: Cytokeratin 7, GFAP: Glial Fibrillary Acidic Protein, TNF: Tumor Necrosis Factor alfa, IL6: Interleukin 6, IL20: Interleukin 20, gal-1: Galectin 1, Gal-3: Galectin 3, Gal-9: Galectin 9, Glut-3: Glucose Tranportator 3, Glut-4: Glucose Tranportator 4, βFGF: Beta Fibroblast Growth Factor, IGF: Insulin Growth Factor, VEGF: Vascular Endothelia Growth Factor, RAR: Retinoic Acid Receptor [34], MMP-9: Matrix Metalloproteinase 9, SHH: Sonic Hedgehog signaling.

Introduction

Craniopharyngiomas (CPs) are uncommon epithelial neoplasms that develop above the sellar turcica of the skull base in the suprasellar, tuberal infundibulum, and third ventricle areas of the brain [1]. These tumors account for 1.2–4.6 percent of all intracranial tumors, with an annual incidence of 0.5–2.5 new cases per million persons across all age categories [2].

Despite their benign histology, these tumors offer several clinical problems [1]. CPs are rare primary brain epithelial tumors with a modest growth rate and symptoms associated to bulk impact and local infiltration of adjacent tissues [3,4], There are two types of CPs, namely, adamantinomatous craniopharyngiomas (AdaCPs) and papillary craniopharyngiomas (PaCPs) [1]. AdaCP affects both children and adults, whereas PaCP affects virtually solely adults [1]. These variations have different histologic characteristics [1]. The significant genomic characteristics of ACPs are somatic mutations of CTNNB1, which encodes β-catenin, as revealed by extensive whole-exon sequencing, while PaCPs are driven by mutation of p. BRAF-v600E [1]. Mutation in exon 3 of CTNNB1, leading to overactivation of the Wnt/β-catenin signaling pathway, is considered the main oncogenic driver of ACP tumorigenesis [1].

The epithelium in AdaCP develops in cords, lobules, and whorls, with palisading peripheral columnar epithelium and loosely organized stellate reticulum. This type is distinguished by "wet" keratin [5]. PaCPs feature well-differentiated monomorphic squamous epithelium covering fibrovascular cores with thin capillary blood vessels and dispersed immune cells including macrophages and neutrophils, and have a smoother surface than AdaCPs, which aids excision. The epithelium lacks surface maturation and there is no "wet" keratin [1].

While columnar epithelium covers the PaCP, significant squamous metaplasia can also occur [6,7]. AdaCP and PaCP also exhibit unique patterns of DNA methylation and gene expression, indicating that they are separate entities [7,8].

The differential genetic backgrounds and epigenetic factors of ACP and PCP lead to differences in targeted therapies. Recently, multiple studies have provided new insight into the tumorigenesis of AdaCP and possible therapeutic targets. The purpose of this research is to investigate papillary craniopharyngioma cases by performing clinical histology, immunohistochemistry, double fluorescence staining, and ultrastructure analysis.

Material and Methods

Patient Population

From 2015 to 2021, we conducted a retrospective and descriptive assessment of medical records of patients who underwent craniopharyngioma surgery at the Neuropathology Department of the National Institute of Neurology and Neurosurgery of Mexico City (INNN). Local ethics committee (C20-88) authorized the study. Two hundred CPs were operated on, with 13 (26%) patients identified with papillary craniopharyngioma from our cohort; pathologically, with complete pre-operation MRI data, were recruited. There were 5 cases of original craniopharyngiomas and 8 cases of recurring tumors or with a history of ventriculoperitoneal shunt. Clinical characteristics retrieved were age, gender, tumor size, symptoms, recurrence, and mortality.

Neuropathology

The histopathological variables analyzed were: cyst formation (CF), squamous metaplasia (SM), inflammation (IM), presence of macrophages (Ma), solid pattern (SP), and brain invasion (BI). Internal portion or basal cells of the vascularized fibroconnective core (BCFVC). In addition, were ranged as; Weak (+) between 1-10 images in the analyzed sample, moderate (++) between 10-25 and strong (+++) more than 25.

Tissue Characterization

During histopathological preparation, the specimens were fixed in formalin and embedded in paraffin. The sections were stained with hematoxylin–eosin (FFPE) tissues from 13 PaCP patients, including 8 recurrent and 5 non-recurrent tumors (13 total subjects), were retrospectively studied, retrieved from the archives of Department of Neuropathology at INNN. Cases were classified according to the revised WHO 2016 classification [1]. The different histological feature or histological components were evaluated; external squamous epithelium (EE), small cell epithelium of the internal portion of the papillary (IPEC), vascularized fibroconnective core (VFC), vessels, epithelium cyst formation (ECF), squamous metaplasia (SM), inflammation, macrophages, inflammatory cells, in the solid pattern (SP), and brain invasion (BI).

The immunohistochemistry was used the PAP method. Primary antibodies used were; CK7, BRAFv600E, clau-1, Clau-5, occludin, E-cadherin, β-catenin, Fascin, Vimentin, GFAP, TNFα, TNFγ, interleukin 6 (IL6), IL (10), IL20, CD68, CD163, Gal-1, Gal- 3 and Gal- 9, Glut-3 and Glut-4, βFGF, IGF, EGFR and PDGF, Ki67 and MVD (CD34) labeling index (li) were performed.

Various primary antibodies expression was evaluated based on the tumor's histological finding components. It was graded based on the intensity of the immunoreaction. The immunohistochemistry detection was grades as negative (-), weak (+), moderate (++), and strong (+++).

Electron Microscopy

Twelve tissue samples were retrieved from paraffin blocks and processed for transmission electron microscopy. Tissue fragments were deparaffinized in Xylol, hydrated with graduated alcohol solutions and cacodylate buffer. Afterward the tissues were post-fixed with 0.5% osmium tetroxide buffer for 1 h at room temperature, washed in the same buffer, alcohol dehydrated and EPON embedded. One fresh tissue sample was fixed in 2.5% glutaraldehyde in 0.1 M cacodylate buffer pH 7.2, alcohol dehydrated and EPON embedded. One μm thick sections (RMC ultramicrotome) were stained with toluidine blue and photographed under a NIKON microscope. Ultrathin sections of 60 nm thickness were contrasted with uranyl acetate and lead citrate, and observed in a Jeol transmission electron microscope (JEM 1400 PLUS; CONACYT 226201).

Results

Clinical Data

This endeavor included thirteen instances: 10 (77%) males and 3 (23%) females, 8 (62%) recurrence and 5 (39%) did not. All of them had radiation. The age range was 18 to 70 years (mean 48years). The onset of symptoms ranged from 6 to 13 months (mean de 1711.54). The duration of the follow-up ranged from 12 to 36 months (mean 22.05). Tumors range in size from 23 to 45 mm (mean de 35.155.3). There were eight recurring tumors and five non-recurrent tumors. Recurrent tumors had a mean age of 44 years, whereas non-recurrent tumors had a mean age of 54 years. Radiotherapy was administered to all patients. Table 1 displays clinical and epidemiologic data.

Neuropathology and Immunohistochemistry Results

The histopathological characteristics of all cases are shown in Table 2. Atypia was correlated with the different histological features (See figure 1). In table 3 are seen the immunohistochemical results of the different primaries antibodies used in relation with the different histological features (see Figure 2 and figure 3, that showed the head map of the immunohistochemical results). Six cases had a cystic appearance. CK7 expression was strongly positive in the SM zone (Figure 3a), BRAF V600E was positive in the membrane form in EE and weakly positive in cells showing SM in nuclear form (3b), claudin 1 was membranal positive immunoreaction in EE (3c), claudin 5 (3d) and occludin (3e) were strong membranal positive reaction in EE and weak in SM (3e). E-Cadherin was both cytoplasmic and membranal positive reaction (1f). β-catenin was positive cytoplasmic in EE positive reaction (3g).

Positive in the basal or internal cells of the CFV. (l) Galectin 1 f was strong cytoplasmic positive reaction in epithelial cells and nuclear immunoreaction in SM. (ll) Gal-3 was weak reaction in cytoplasm in SM. (m) Galectina 9 weak positive expression in SM and apoptotic changes, and in (n) Glut-3 was in the endothelial cells (IHQ x400).

βFGF was weak positive reaction in BCFV C (3h), IGF (3i), and EGF(3j) were cytoplasmic positive immunoreaction in EE and nuclear in SM, and DPGF was positive immunoreaction in BCFVC (3k).

Gal-1 was strong cytoplasmic positive immunoreaction in EE and nuclear expression in SM (3l), Gal- 3 was weak positive cytoplasmic reaction in SM (3ll), and in the ECs, and Gal-9 was only positive in cells with apoptotic changes (3m), Glut-4 wa s negative in all histological features.

TNFα was weak positive reaction in BCFVC (Figure 4a), TNFγ (4b), fascin (4c) and il6 (4d) was positive in BCFVC, il10 (4e), il 20 (4f) were positive in SM. CD68 was positive in macrophages in

Table 1: Clinical and epidemiological data, according each case.

	Age	Gender	Symtopms	Recurrence	RadioTx	Folow-up	Tumor size	Dead
Case1	18ys	Male	1,2,3	----	+	31mm	32mo	no
Case2	25ys	Female	1,2,3	----	+	34mm	25mo	no
Case3	36ys	Male	1,2,3	+	+	36mm	24m0	no
Case4	45ys	Male	1,3,4	+	+	37mm	35mo	no
Case5	67ys	Male	1,2,3,5,	----	+	32mm	36m0	no
Case6	54ys	Male	1,2,4,5	----	+	34mm	26mo	no
Case7	54ys	Female	1,2,4,5	----	+	23mm	16mo	yes
Case8	56ys	Female	1,3,4	+	+	41mm	18mo	no
Case9	44ys	Male	1,2,3,4,6	+	+	34mm	22mo	yes
Case10	49ys	Male	1,2,3,4	++	+	45mm	12mo	no
Case11	67ys	Male	1.2.3,5	++	+	36mm	20mo	yes
Case12	56ys	Male	1,2,5,6	+	+	34mm	17mo	yes
Case13	70ys	Male	1,2,3,6	++	+	40mm	12mo	yes

--- (non), (+) yes, (++) two times, clinical symptoms; cefalea (1), visual disturbance (2), endocrine alteration (3), insipid diabetes (4), arterial hypertension (5), obesity (6). ys= years; RTx= radiotherapy; mo= months.

Table 2: Histopathological features according in each one of the cases.

	Atypia	SM	IM	Ma	CF	SP	BI	Ki67-Li	CD34
Case 1	---	+	+	+	----	+	---	4%	12%
Case 2	---	+	--	+	----	+	---	4%	14%
Case 3	---	---	--	---	---	+	---	5%	12%
Case 4	---	---	--	+	---	+	---	5%	13%
Case 5	---	---	--	---	---	+	---	4%	12%
Case 6	+	--	--	+	---	++	---	3%	15%
Case 7	+	+	--	---	---	++	---	4%	15%
Case 8	+	++	--	+	+	++	+	7%	16%
Case 9	+	+	+	+	+	++	++	8%	19%
Case10	+	+	+	+	+	++	++	9%	18%
Case 11	+	++	+	+	++	++	++	9%	18%
Case 12	+	+	++	+++	++	++	++	10%	21%
Case 13	+	++	++	+++	++	+++	++	11%	20%

(SM) Squamous metaplasia, (Im). inflammation, (Ma) macrophages, (CF) cyst formation, (SP) solid pattern, brain invasion (BI), Ki-67li (Ki67 labeling index) Microvascular density (MVD).

Table 3: Showed the immunohistochemsitry resylts in relation ship the histological features.

Primaries antibodies used	Source	EE	IE	SM	FVC	CA	CP	SP	EC	Ma
CK7	DAKO	--	---	+++	----	----	----	----	----	----
	Clone OV-TL12/30 M7018									
BRAFv600E	BSB 2827	++	+	+	---	+	--	++	---	---
Claudin1	Genetex	+++	+	--	---	+	++	++	---	---
	GTX15098									
Claudin 5	(A-12): sc-374221	++	--	++	---	---	++	---	---	---
Occludin	sc133256	++	+	--	--	+	+	++	---	---
E-cadherin	Biogenex MU390-UC	+++	++	---	---	---	+	---	---	---
Beta catenin	sc-419477-ACT	++	+	---	----	+	++	+	--	---
βFGF	Biocare	++	+	--	---	+	+	++	---	---
	AM3595M									
IGF-1	(H-9): sc-518040	---	+	+++	---	+	++	---	---	---
EGFR	Biogenex	+	++	+	---	----	++	----	---	---
	PU335-UP									
PDGF	Biogenex MU376-UC	+	++	+	----	---	---	---	---	---
Gal1	(C-8): sc-166618	++	+++	--	----	+	+	++	---	---
Gal 3	(M3/38): sc-23938	++	+++	--	---	+	+	++	---	---
Gal 9	(B-9): sc-271533	--	---	+	+	+	+	---	---	---
Glut-3	GTX15311	+	--	++	----	+	+	++	+	----
Glu-4	(IF8): sc-53566	---	---	---	----	----	----	----	----	----
Facin	BIOGENEX	---	----	++	+	---	---	---	---	----
	MU488-UC									
IL6	EPR21710] (ab229381	+	---	++	+	---	++	---	+	++
IL10	A40526	+	---	+	----	---	+	---	---	+
IL20	A11996	+	---	++	+	---	++	---	+	++
TNFα	(TN3-19.12): sc-12744	+	---	---	+	---	++	---	---	+
TNFγTNFk	(D-2): sc-8041	+	----	----	----	----	++	----	----	+
CD68	Biogenex MU390-CP	+	+	---	+++	---	---	+	+	+++
CD163	CS33715	---	+	--	+	---	---	+	---	+
Vimentin	Biogenex	+	+	----	----	----	+	---	+	+
	MU-074-UC									
GFAP	Biogenex	---	----	++	----	---	---	---	---	---
	MU-020-UC									

Immunoexpresion of the primary antibodies used was calculated in the different histological features according immunoreaction: negative (--), weak (+), moderate (++) and strong (+++). External epithelium (EE), internal epithelium (IE), squamous metaplasia (SM), fibrovascular core (FVC), cellular atypia (CA), cyst pattern (CP), solid pattern (SP), endothelial cells (EC), Macrophages (Ma). cytokeratin 7(CK7), Glial fibrillary acidic protein (GFAP). Tumor necrosis factor alfa (TNFα), interleukin 6 (IL6), interleukin 20 (IL20), Galectin1 (gal-1), Galectin 3 (Gal-3) and Galectin 9(Gal-9), Glucose Tranportator 3 (Glut-3) and Glucose Tranportator 4 (Glut-4), beta fibroblast growth factor (βFGF) and Insulin growth factor (IGF), KI67(BIOGENEX MU370-UC). Dilution 1:100.

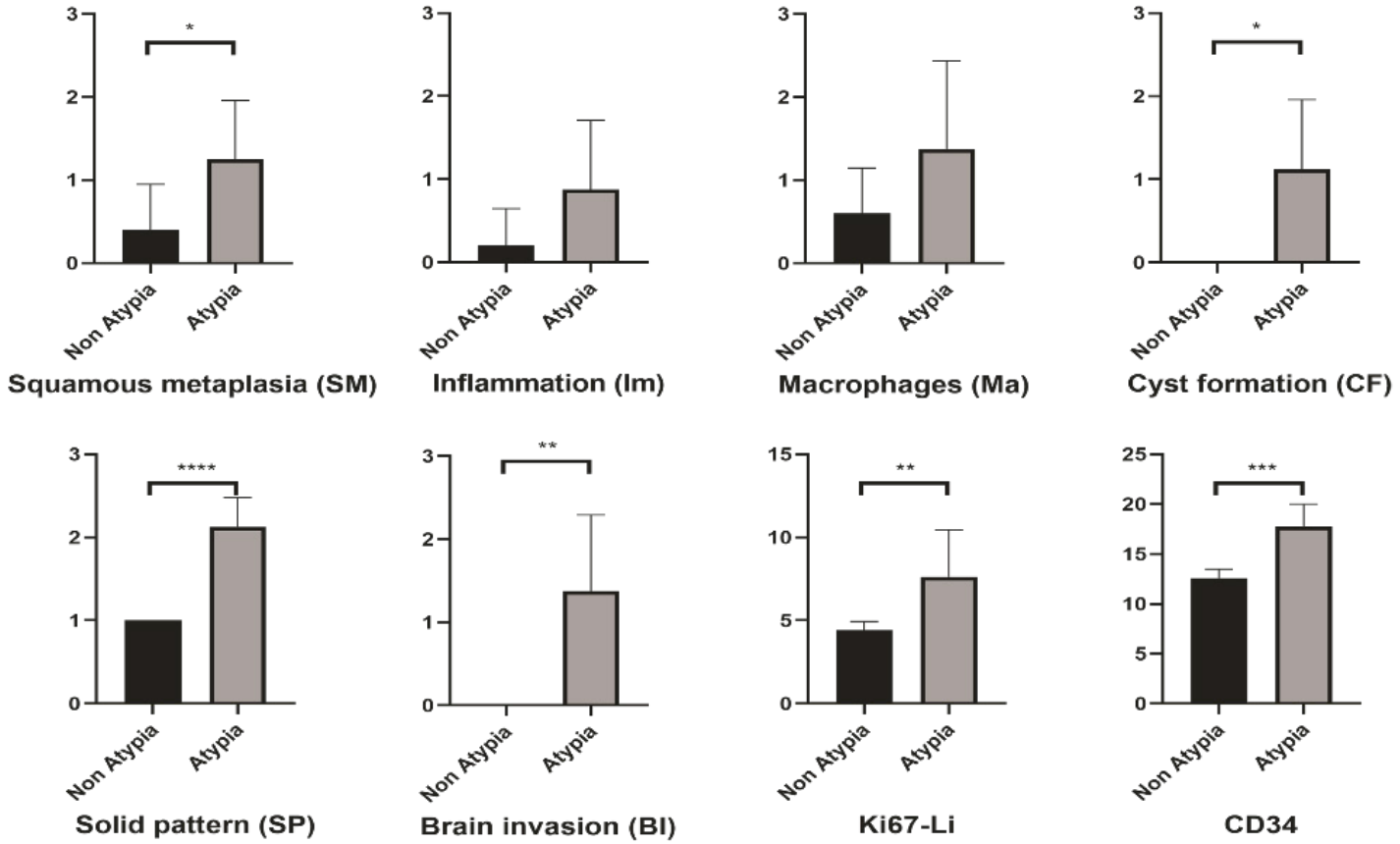

Figure 1: Showed the histograms of the cellular atypia in relationship with squamous metaplasia, inflammation, macrophages, cyst formation, solid pattern, brain invasion, Ki-67li, and MVD.

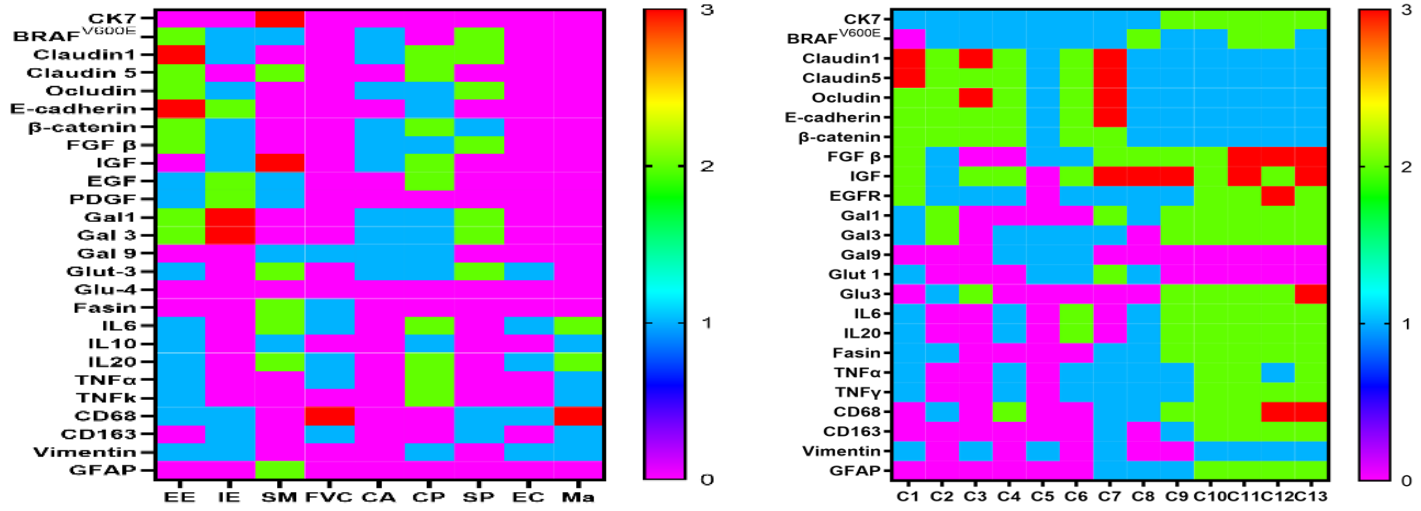

Figure 2: Showed the head map of the differents proteins expression accoring histological features in (a) and relation ship each one of the case.

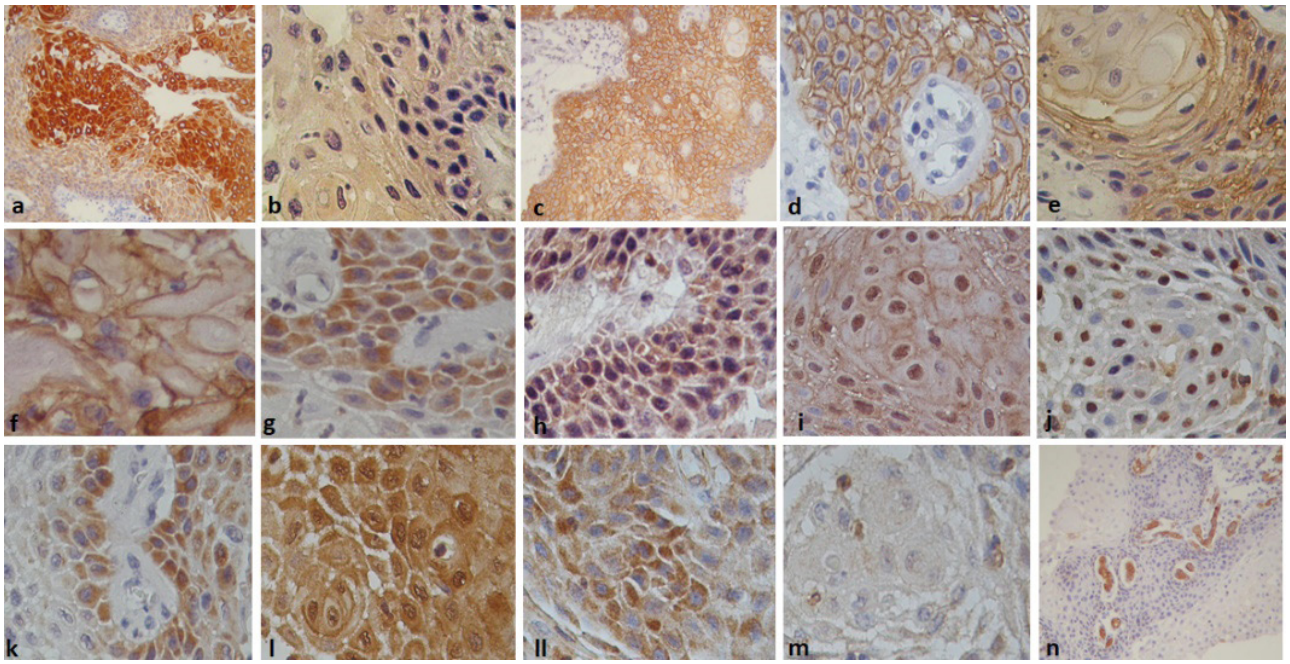

Figure 3: Immunohistochemistry. (a) CK/7 positive immunoreaction in squamous metaplasia. (b) BRAF V600E, was positive in epithelial cells membrane and SQ nuclear expression. (c) claudin 1 positive membranal immunoexpresion, (d) claudin 5 immunoexpression, (e) occludin positive, (f). E-Cadherin citoplásmica immunoexpression, (g). N-cadherina membranal expresión and in (g) La beta catenin positiva immunoexpresion. (h) βFGF weak immunoexpresion, (i) IGFR was nuclear positive SM. (j) EGFR showed positive cytoplasmic and nuclear expression. And in (k) DPGF was Figure 4. The heat map of the proteins expression with the different histological features in (a) and heat map of the proteins expression in relationship with each case in (b).

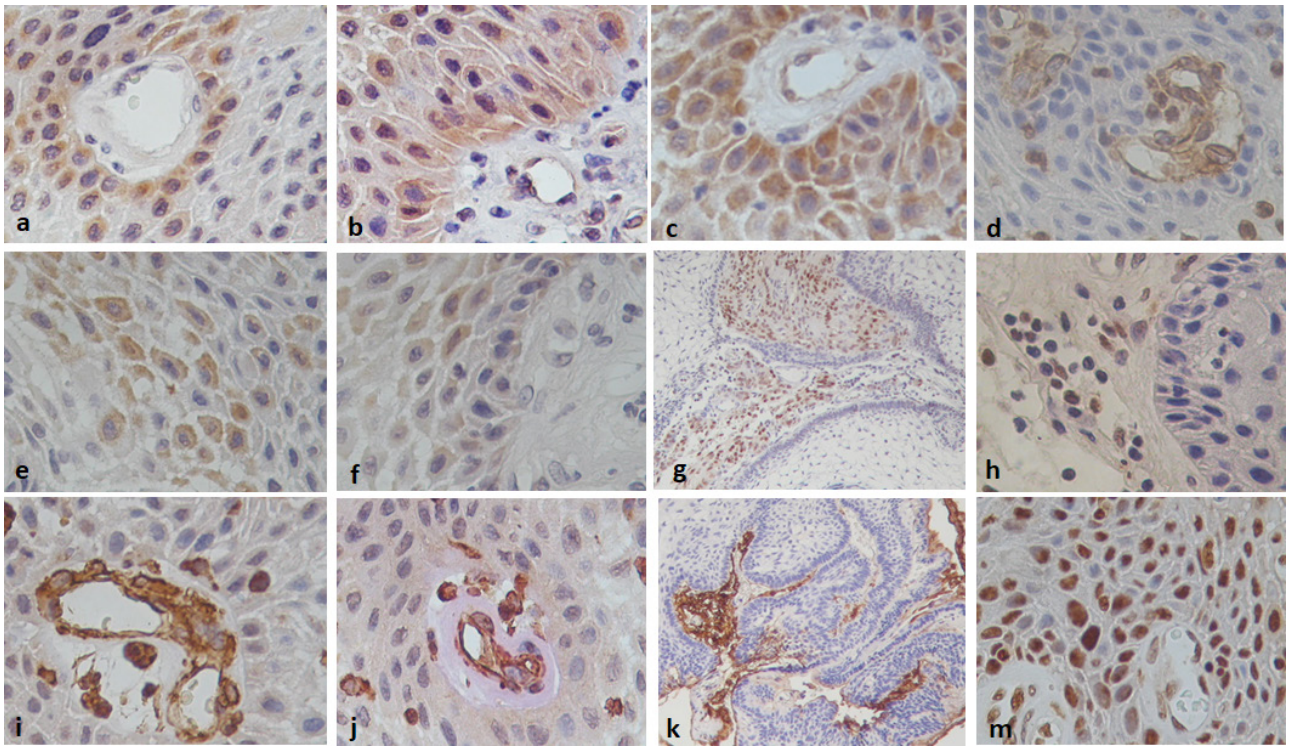

Figure 4: Immunohistochemistry. (a) TNFα was immunoreaction in the basal internal cells of the fibrovascular central core (b) TNFγ and fascin in (c) were immunoreaction positive epithelial cells and squamous metaplasia. (d) Showed il6 positive expression in internal or basal epithelial cells and in the endothelial cell of the fibroconective vascular central core. (e) and (f) il20 was positive in squamous cells, (g) showed the CD68 immunoexpresion in macrophages of the FVC (x200), and in (h)observed few CD163 macrophages positive. (i) Vimentin positive reaction in the wall of the vessels. (j) Con la tinción de PAS +vimentina (observamos engrosamiento de la membrana basal vascular(k) GFAP pone en evidencia la infiltración al tejido cerebral. In addition, in (m) Ki67 nuclear immunoexpressing (x400).

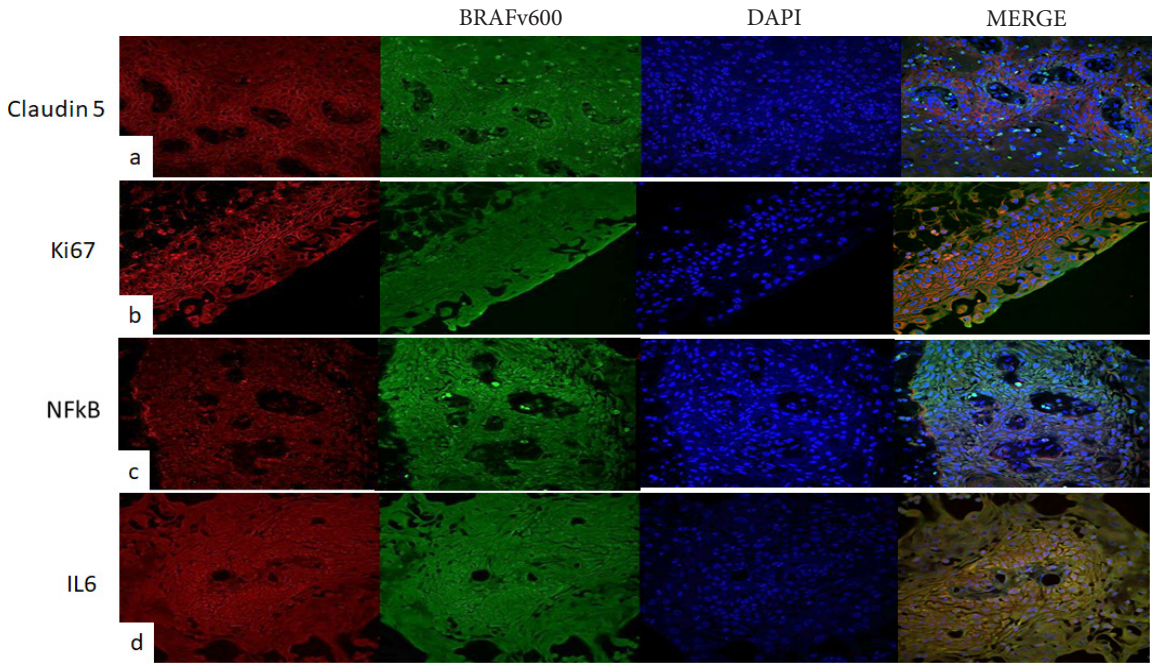

Figure 5: Doble fluorescence (a) observed claudin 5 (red) with FRAFv600 in (green), DAPI (blue). observed merged cooexpresio n (b) Ki67 (red) and FRAFv600 immunoexpression (green), DAPI (blue) and we observed high cooexpresion in © TNF a in (red) and FRAFv600 (green) both cooexpresion and in (d). iL6 expression in (red) and FRAFv600(green), DAPI in (blue). And merge cooexpresion.

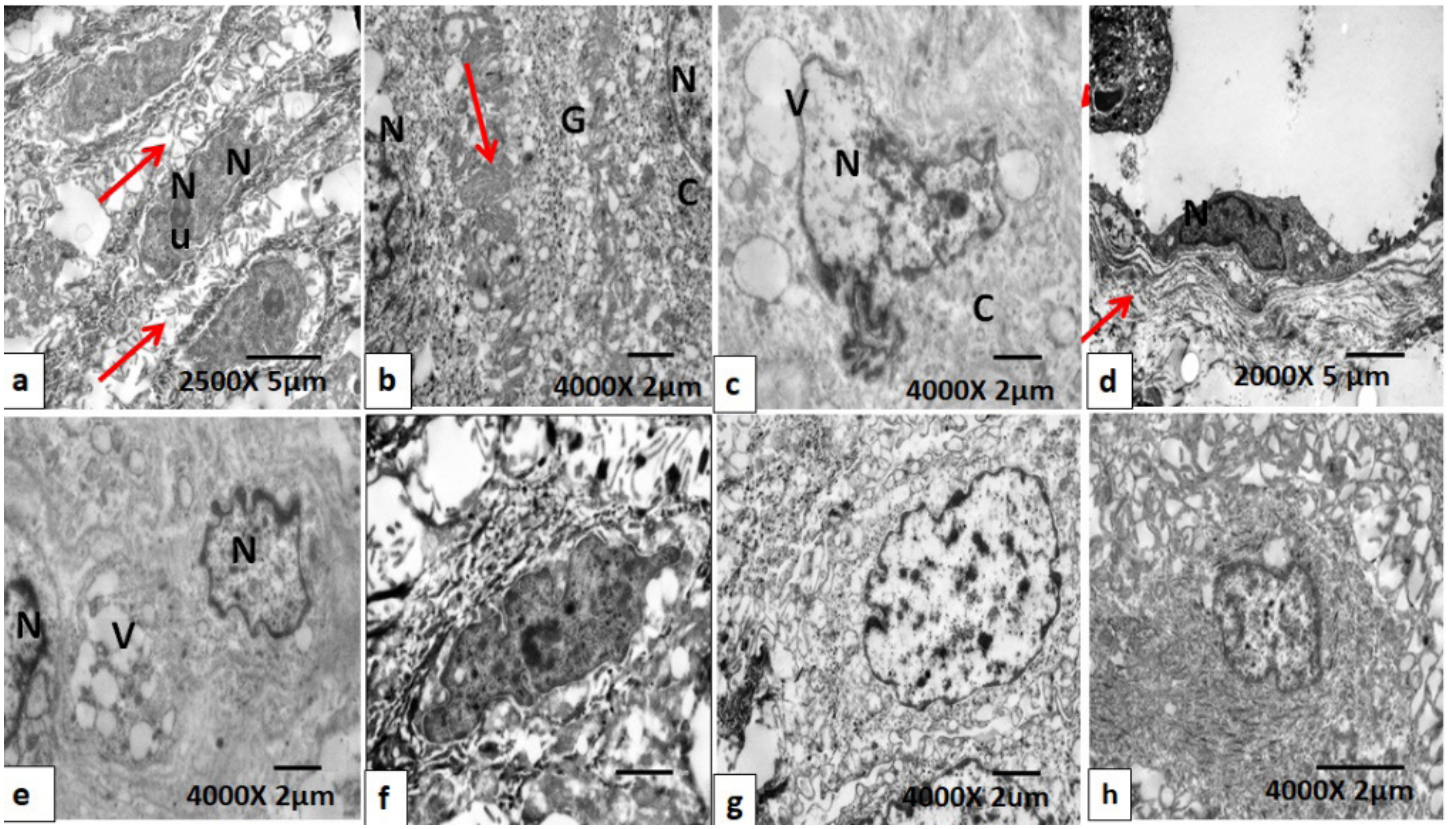

Figure 6: Transmission electron microscopy micrographs showed cytoplasmic vaculae and glycogen position in the epithelium cells (a and b), where the cells show misshapen cell nucleus and vacuoles with oily material (c). Endothelial Cells (d) and vessels surrounded by fibroconnective core showed intermediate filaments disorganization (e). Squamous metaplasia cells show loss of intercellular junctions (f), with abundance of electron dense granules (g) and nuclear loss of chromatin and poor differentiated cytoplasm and alteration in cellular processes in cell-cell adhesion in (h). Uranyl acetate-and Lead citrate stain.

FVC (4g), and in occasional cells intro EE and CD163 was positive in few cells (4h). Vimentin was positive in the vascular wall (4i), and with PAS +vimentin we observed a vascular basal membrane (4j). GFAP showed the brain invasion (4k). Ki-67li was nuclear positive immunoreaction (4m).

Ki-67li was 6.31±3.0% (range, 3-11%), in recurrence (mean 8±.945, median 9) compared non-recurrence (3.60±.245 median 4%). We observed a statistically significative differences correlation ship between Ki67-li with recurrence, atypia, solid pattern, and immunoexpresion with CK7, glut3, il6, il20, TNFa, TNFγ and CD68. MVD mean range was of 17.31±3.4 (mean range 12-22%), recurrence (mean 19.63±.680) vs non-recurrence (mean of 13.60±.678). We observed a statistically significative differences correlation ship between MVD and recurrence, atypia, cysts pattern and macrophages, and Glut3, Gal3, TNFa, TNFγ and CD68 immunoexpresion.

We observed statistically significative differences in the correlation between atypia with SM, Ki-67li, and MVD. BRAFV600E regarding tumor size, inflammation, brain invasion, cyst patter, macrophages, CK7, claudin 5 and occludin, Glut3, Gal3, iL20, TNFa, CD68 with CD163 positive immunoexpresion with higher Ki-67li and MVD. Clau-5 was correlated with the age of patients, atypia, solid pattern, occludin, E-cadherin, glut-1, il6, and TNFa immunoexpression. However, in recurrent patients a diminished expression was found.

With the double fluorescence staining we observed a co-expression between Claudin 5 and BRAFv600 (Figure 5a), inferring that the higher BRAFv600E expression, the lower Claudin 5 (5b) observed. We also found a higher expression of BRAF V600E with TNFα in (5c) and BRAFv600E with IL6 cooexpresion in (5d).

Electron Microscopy

Ultrastructure analysis revealed cytoplasmic vacuoles and glycogen positions in epithelial cells (Figures 6a and 6b), with the cells displaying a malformed cell nucleus and vacuoles containing oily substances (6c). Disorganization of intermediate filaments was seen in endothelial cells (6d), and arteries surrounded by a fibroconnective core (6e). Squamous metaplasia cells have a lack of intercellular connections (6f), an abundance of electron dense granules (6g), and chromatin loss in the nucleus, and poorly differentiated cytoplasm (6h).

Discussion

Craniopharyngiomas are associated with substantial morbidity. Although, CPs can be highly aggressive and have a tendency to recur following surgical removal, the literature indicates that it seldom establishes malignant behavior [5]. Aggressive behavior of the tumor is reflected by its tendency towards damaging of adherent structures [7].

Many studies are designed for discriminating clinical, morphological, ultrastructural and immunohistochemical prognostic factors of recurrent PCs using the expression of proteins from p53, p63, p73 [1], and growth hormone receptors presence, as well as IGF-1 receptors, somatoliberin receptors, estrogen receptors, progesterone receptors and leptin receptors, vascular, VEGF, RAR cathepsins, MMP9, collagen IV, CXCL12/CXCR4, Sonic Hedgehog signalling pathway, SOX9, CD166, oncogenes BRAF/CTNNB, and β-catenin [9] and furthermore the presence of Rosenthal fibers, MVD and Ki-67li [10]. Are using with as a prognostic predictor factor.

It has been seen that Ki-67li has been one of the most important factors to predict growth, invasion and recurrence. Ki-67li in CPs is low in both histological types. However, it is higher in AdaCPs than in PaCPs. On average it is 3%. In our findings, the median Ki-67li in recurrent CPs (9.0%) was not significantly different from that of non-recurring tumors (7.9%) and was significantly higher in tumors with a heavy inflammatory reaction and diabetes insipidus at presentation [10]. We observed higher Ki-67li in association with recurrence, atypia, solid pattern, and immunoexpression with CK7, glut-3, IL6, IL20, TNFa, and CD68. However, contradictory data has been published. According to several authors, Ki-67li is not a prognostic factor of tumor's relapse. Thus, is not a reliable prognostic factor of CPs recurrence [10]. Tumor's angiogenesis is of prognostic value in patients with CPs [11]. In our results, there was a correlation between MVD and recurrence, atypia, solid and cysts pattern and macrophages, cyst pattern and glut3, Gal3, TNFa y CD68 immunoexpresion [11].

In this study, we analyzed different markers that participate both in the epithelial membrane (claudins, occludin, β-catenin, E-cadherin) as well as in the cells of the internal epithelium of the FVC with in the cells that present differentiation towards SM. There were no differences in the CK7 expression between recurrent and non-recurrent tumors. However, recurrence tumors had loss of adhesion molecules (claudins, occludin, β-catenin, E-cadherin) expression and high immunoreaction of βFGF, DPGF, IGF and EGFR. The recurrent tumors also expressed higher immunoreaction of TNFa, TNFγ, CD68 y Il6, Il20 and loss of expression of CD163.

PaCP lacks nuclear β-catenin accumulation [12], and can be supportive in the differential diagnosis between both AdaCP and PaCP in the setting of small biopsies [13]. Moreover, the restricted nuclear β-catenin accumulation in the cohesive cell clusters within the whorl-like areas supports that aberrant β-catenin expression may play a role in the morphogenesis of AdaCP [12]. We observed that β-catenin expression was membrane and focally cytoplasmic in the internal epithelium of the papillary structure and unclear expression in changes of SM.

The BRAFV600E mutation causes the mitogen-activated protein kinase (MAPK) pathway to be activated [13]. The MAPK pathway is a significant intracellular signaling route that regulates cellular proliferation, gene expression, differentiation, mitosis, cell survival, and death [14]. Multifunctional protein that interacts with the cytoskeleton in a variety of ways. In vitro, the mutation is a driver

mutation, and when BRAF V600E was ectopically produced in fibroblast cell lines [14,] it induced hyper activation of the MAPK cascade and malignant transformation to targeted treatment with the combination of Dabrafenib and Trametinib. The V600E mutation causes the MEK-ERK pathway to be activated [14]. β-catenin is localized at the cell membrane adhesion complexes, although the intracellular cytoplasmic levels are reserved very low, because of its association with several proteins, APC, GSK-3β, β-TrCP, and axin/conductin, which direct cytoplasmic β-catenin to proteasome-mediated degradation [13,14]. Wnt pathway activation leads to GSK-3β inhibition activity, which results in the blockade of the β-catenin phosphorylation and the consequent stabilization of cytoplasmic β-catenin, which eventually translocated to the cell nucleus and transcriptional activation of target genes [12].

We observed a correlation with the expression of BRAFV600E with tumor activity higher Ki-67li and MVD, strong expression of growth factors (βFGR, IGFR, EGF, DPGR), GLUT3, Gal 1, 3, and 9, markers of inflammation (TNFα, TNFγ, IL6, IL20) and macrophages (CD68 and CD163) and loss of membranal TJ proteins expressed in endothelial and epithelial (claudins, occludin, β-catenin, E-cadherin) [15]. With they play an important role in cell polarity and cell adhesion as well as in maintaining paracellular barrier functions [9,15,16]. Furthermore, areas with distinct squamous epithelial differentiation showed a weaker staining pattern compared with adjoining epithelial layers, cystic tumor areas with fibrotic degeneration and blood vessels were always negative.

Different types of CPs cells have been observed and described by ultrastructure [14]. The cells are densely packed into stratified epithelial clumps with a large, oval-shaped, slightly deformed nucleus and an integrated, but rugged nuclear membrane, as well as abundant tonofibrils and mitochondria, rough endoplasmic reticulum, ribosomes, and microvilli on the cell surface, and the cells are loosely arranged with a vast cell gap in which integrated intercellular desmosomes and multiple connections appeared to have formed [14]. The CPs cells' nucleus, showing a high degree of protein synthesis [17]. Indicating vigorous metabolism and well-developed rough endoplasmic reticulum and ribosomes, as seen in fully differentiated and actively working cells [16]. Tonofibrils and microvilli are abundant, suggesting active cell contraction, which includes movement, cytoplasm flow, phagocytosis, and excretion [17]. Primary cilia are seen throughout the neoplastic epithelium of AdaCP, but are only found in basally orientated cells in the fibrovascular stroma in PaCPs [17], and cilia-dependent hedgehog signaling is involved in the pathogenesis of CPs [16]. However, FOXJ1 expression discriminates Rathke's cleft cysts from entities in the sellar/suprasellar region with overlapping histologic features such as CPs [18].

By ultrastructure, we observed intracytoplasmic vacuole binding proteins, glycogen deposits and an increase in microgranules [17]. The above could be related to the process of paracrine secretion and cellular senescence in promoting tumorigenesis [19]. Since little is known about the secretory activity of these tumors, more studies should be carried out to confirm this event. The OMF can be secreted by these tumors, the conditions of his presence and/or absence are unknown as well as, its prognostic value. However, some and further studies are needed to confirm this hypothesis.

Conclusions

From this case study, we can foresee PaCPs' clinicopathological behavior. However, our sample limits the scope of our findings. Only 13 cases that are not enough to be able to conclude or adequately elucidate our results. We understand that the sample may be very limited.

References

1. Louis DN, Ohgaki H, Wiestler OD, et al. WHO Classification of Tumours of the Central Nervous System. International Agency for Research on Cancer. 2007; 238-240.
2. Prabhu VC, Brown HG. The pathogenesis of craniopharyngiomas. Childs Nerv Syst. 2005; 21: 622-627.
3. Caijie Qin, Wenxing Hu, Xinsheng Wang, et al. Application of Artificial Intelligence in Diagnosis of Craniopharyngioma. Front Neurol. 2022; 12: 752119.
4. Zihao Zhou, Sheng Zhang, Fangqi Hu. Endocrine Disorder in Patients with Craniopharyngioma. Front Neurol. 2021; 12: 737743.
5. Elarjani T, Alhuthayl MR, Alhindi H, et al. The effect of radiation therapy and chemotherapy on malignant craniopharyngioma: A review. Surg Neurol Int. 2021; 12: 539.
6. Martinez-Barbera JP, Andoniadou CL. Biological Behaviour of Craniopharyngiomas. Neuroendocrinology. 2020; 110: 797-804.
7. Capper D, Preusser M, Habel A, et al. Assessment of BRAF V600E mutation status by immunohistochemistry with a mutation-specific monoclonal antibody. Acta Neuropathol. 2011; 122: 11-19.
8. Priscilla K Brastianos, Sandro Santagata. BRAF V600E mutations in papillary craniopharyngioma. Eur J Endocrinol. 2016; 174: R139-R144.
9. Garcia-Lavandeira M, Saez C, Diaz-Rodriguez E, et al. Craniopharyngiomas express embryonic stem cell markers (SOX2, OCT4, KLF4, and SOX9) as pituitary stem cells but do not coexpress RET/GFRA3 receptors. J Clin Endocrinol Metab. 2012; 97: E80-E87.
10. Moszczyńska E, Prokop-Piotrkowska M, Bogusz-Wójcik A, et al. Ki67 as a prognostic factor of craniopharyngioma's recurrence in paediatric population. Childs Nerv Syst. 2020; 36: 1461-1469.
11. Vidal S, Kovacs K, Lloyd RV, et al. Angiogenesis in patients with craniopharyngiomas: correlation with treatment and outcome. Cancer. 2002; 94: 738-745.

12. Cao J, Lin JP, Yang LX. Expression of aberrant β-catenin p-63 in craniopharyngioma. Br J Neurosurg. 2010; 24: 249-256.
13. Brastianos PK, Santagata S. Endocrine tumors: BRAFv600e mutations in papillary craniopharyngioma. Eur J Endocrinol. 2016; 174: R139-R144.
14. Brastianos PK, Shankar GM, Gill CM, et al. Dramatic Response of BRAF V600E Mutant Papillary Craniopharyngioma to Targeted Therapy. J Natl Cancer Inst. 2015; 108: djv310.
15. Swisshelm K, Macek R, Kubbies M. Role of claudins in tumorigenesis. Adv Drug Deliv Rev. 2005; 57: 919-928.
16. Christina Stache, Annett Hölsken, Rudolf Fahlbusch, et al. Tight junction protein claudin-1 is differentially expressed in craniopharyngioma subtypes and indicates invasive tumor growth. Neuro Oncol. 2014; 16: 256-264.
17. Coy S, Du Z, Shue SH, et al. Distinct Patterns of Primary and Motile Cilia in Rathke's Cleft Cysts and Craniopharyngioma Subtypes. Mod Pathol. 2016; 29: 1446-1459.
18. Zhu J, Chao Y. Craniopharyngioma: Survivin expression and ultrastructure. Oncol Lett. 2015; 9: 75-80.
19. Gonzalez-Meljem JM, Apps JR, Fraser HC, et al. Paracrine roles of cellular senescence in promoting tumourigenesis. Br J Cancer. 2018; 118: 1283-1288.